EAI Endorsed Transactions
on Energy Web

Research Article EAI.EU

Evaluation of MPC-based arctan droop control strategy in islanded microgrid

J.D.D. Iyakaremye [1,*], G.N. Nyakoe [2] and C.W. Wekesa [1]

[1] Department of Electrical Engineering, Pan African University Institute for Basic Sciences, Technology, and Innovation (PAUSTI), P.O. Box 62000-00200, City Square, Nairobi, Kenya
[2] Department of Electrical Engineering, Jomo Kenyatta University of Agriculture and Technology (JKUAT), P.O. Box 62000-00200, City Square, Nairobi, Kenya

Abstract

The microgrid (MG) is an emerging technology for supplying energy from renewable energy sources (RES). Due to their intermittent nature, RES require an inverter and smooth operation control system when integrated into an MG. Conventional droop control is commonly used in microgrid control but cannot achieve adequate power-sharing when output impedances of inverters are different; thus, enhancing its performance is required. This paper's main objective is to design a finite control set model predictive control (FSC-MPC) based arctan droop control and evaluate its performance against the conventional droop control strategy. The proposed control technique guarantees a strong transient response when there is a dynamic load change during MG operation. The results showed that the proposed control strategy ensures proportionate power-sharing of paralleled voltage source inverters with unequal line impedances than the traditional droop controller, which can vary.

Keywords: Arctan droop control, model predictive control, power-sharing, comparative evaluation, microgrid.

Received on 24 November 2020, accepted on 08 February 2021, published on 19 February 2021

doi: 10.4108/eai.19-2-2021.168724

1. Introduction

Distributed generation (DG) is increasing in many parts of the world. DG's high penetration to the electric network gives rise to the microgrid (MG) concept. It is defined as a cluster of DG units, such as (solar photovoltaics, mini generators, power cells, wind turbines, fuel cell systems), electric storage units, and loads [1]. The integration of Res to the microgrid requires a voltage source inverter (VSI) and its associated controls for better operation. A microgrid can be grid-connected or in an islanded mode of operation [2].
When the microgrid satisfies the electricity demand utilizing the primary grid, it is called the grid-connected mode. When its local generation provides the demand, it is called islanded or autonomous mode. In grid-connected mode, a controller's main objective is to meet the energy demand. Its main aim is to provide frequency, voltage control, and ensuring energy support in islanded mode. When there are no synchronous generators for balancing demand and supply for island service, the inverter must provide these controls, mainly frequency control. DGs boost service efficiency and eliminates the cost of generation growth planning. It expands the probability of islanding microgrid sources in charge of local power generators' quality factors, which is impossible for traditional controlled power production [3].

The VSIs need to have adequate control for different DGs' proper operation in a microgrid to generate the same frequency. Monteiro et al. [4] proposed an enhanced voltage control using a pulse width modulation with a multi-loop control method to control electric vehicle operating as an uninterruptible power supply (UPS) in a smart home. The purpose was to supply a sinusoidal voltage for linear and nonlinear electric loads. Guerrero et al. [5] demonstrated that the incorporation of linear cascaded control could hamper droop control's efficacy.

Some researchers proposed centralized control using communication links. Nonetheless, it is expensive to use

*Corresponding author. Email: iyakjdd@gmail.com

them in remote areas with a considerable distance between VSIs. Decentralized controls are being studied to overcome the drawbacks of the communication control links. The droop control strategy gained popularity and is widely used in microgrids control because it does not require any communication link and is simple to implement. Droop controls assure power equitability for DG units in a microgrid network. However, they showed some limitations like inadequacy in reactive power-sharing and poor voltage regulation.

2. Literature review

Tayab et al. [6] made a detailed analysis of the latest droop studies, introduced and explained the control strategy, and revealed that it is difficult to adjust a common control technique for all purposes or boost the limitation of modern droop control by one modification. They demonstrated that frequency stability and appropriate active power-sharing are ensured by conventional droop control; however, it causes reactive power-sharing errors. Many researchers have done extensive research on droop control and its derivatives to prove its adequate control of VSIs. Manjunath et al. [7] noted that using the arctan frequency droop method reduces the steady-state frequency variance and raises the settling time. Margoum et al. [8] used droop control and virtual impedance loops as the primary control for adequate power-sharing between two parallel-connected VSIs; along with the secondary control loops, the control strategy can clear the magnitude and frequency deviations caused by the primary control.

The quadratic droop controller was proposed in [9], a modified version of traditional droop to control voltage and frequency in islanded VSIs based microgrid; the controller's power-sharing features showed that the controller interpolates between low-gain and high-gain power-sharing. Hennane et al. [10] proposed an improved droop control method that considers synchronization and power-sharing of different DGs in various PCC islanded microgrids. At the same time, the real features of the line feeders are considered in the control design. Chen et al. [11] proposed a control strategy that consisted of FSC-MPC with a capacitor current estimator for voltage reference tracking and virtual resistance droop control for power-sharing.

Bouzid et al. [12] also proposed a new droop control based on a decoupled trigonometric saturated (DTS) controller to ensure the power-sharing in a meshed parallel inverter system. FCS-MPC was used by [13] as a control method based on explicit tracking of the derivative's reference voltage to regulate the voltage at a common bus; this method also used a simple droop controller for power-sharing among the VSIs. Babqi et al. [14] used MPC as a primary control, droop control as a secondary control; both were used to regulate the output voltage and frequency of each DG-based VSI in an autonomous microgrid. Tayab et al. [15] proposed a modified traditional droop control strategy where the derivative term in the active power loop was added to the conventional droop to improve the transient response and decrease the frequency deviation. The proportional-integral (PI) term and the root mean square value of VSI output voltage in the reactive power loop were added to the traditional droop that reduces the effects of the line impedance disparity and attains precise reactive power-sharing among parallel-connected VSIs and restricts the voltage deviation.

To the best of the author's knowledge and based on the literature cited above, none have designed the MPC-based arctan droop control strategy and its comparative evaluation with the conventional droop control method. In this paper, a control strategy was designed to control the paralleled VSIs to assure the MG's proper control. Therefore, the MPC-based arctan droop controller with virtual impedance is used to ensure voltage and frequency stabilization; moreover, the power equitability among the microsources is confirmed. Each part of this hybrid control strategy provides adequate energy management and MG operation. Thus, it includes the virtual impedance to balance lines impedance. The arctan droop control method used in the proposed control technique eliminates the droop slope of constant frequency and replaces it with an algorithm based on the arctan function. Enforcing this arctan-based power profile, the microgrid operator will guarantee that the microgrid operating frequency is still within preset limits [16]. For its excellent transient performance, the FCS-MPC strategy is used to boost voltage reference tracking performance and reduce complexity compared to the traditional cascaded linear control method, which uses a multi-loop control scheme [11]. This paper shows the MPC-based arctan droop control method's effectiveness in tracking the voltage reference and continuously keeping the preset limits' frequency versus conventional droop control strategies where the voltage and frequency may vary.

The paper is arranged as follows: a brief literature review is given in section 2; the alternating current (AC) microgrid structure is presented in Section 3. Section 4 sets out the proposed control methods and parameters critical indicators for a better control strategy for parallel-connected VSIs in a microgrid. Results and discussions are presented in Section 5, and, finally, Section 6 summarizes the conclusions.

3. Description of the system

Figure 1 displays an AC microgrid. It is composed of two DG units connected in parallel via VSI. As the DGs are usually attached to the energy storage system (ESS) to ensure a reliable supply chain, it is assumed that the inputs of the VSIs are direct current (DC) [17]. The load power is shared via a standard AC bus. It is possible to connect such microgrids to the primary grid or to operate in an autonomous mode. Droop control is generally used because it procures sufficient power-sharing capability between different modules, as the control is done locally.

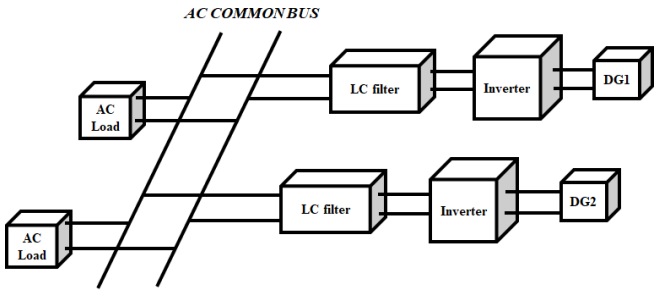

Figure 1. Microgrid-based VSIs in islanded mode [11]

During this research, the authors analyze MPC-based arctan droop control's performance evaluation and compare it to traditional droop control for VSIs based microgrid. The comparison takes into consideration reactive and active power sharing errors, voltage deviations, and frequency deviations.

4. Methods

4.1. Voltage and current loop control

The arrangement of microgrid (MG) used in this paper is seen in Figure 2. This MG is composed of two DGs. Each DG is assumed to have a battery attached to it to provide constant DC voltage. DGs are connected to the load employing LC filters and output impedances. It is assumed that the MG operates in an autonomous mode. The specifications for the microgrid are summarized in Table 1.

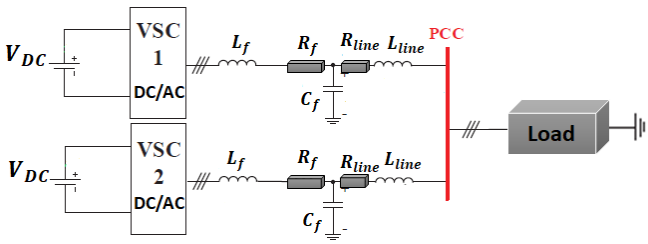

Figure 2. VSI system in an MG

The specification of each VSI and the inner loop controllers for the voltage and frequency droop controller is shown in Figure 3, where:

Ll_f : Filter inductor
Rl_f : The series resistance of the filter inductor
C_f: Filter capacitor
R_T : Line output resistance
L_T : Line output inductance
V_f : Capacitor voltage
I_T : Output current

The primary role of inner control loops at the low control level of current and voltage is to determine the DG units' operating state. This level customarily guaranteed operating conditions like system stability and fast response.

The internal loop output produces the switching signals in VSI.

By using dq transformations, the current and voltage dynamics are expressed as follows:

$$\begin{cases} E_d = Ll_f\left(dI_{df}/dt\right) - \omega Ll_f I_{qf} + I_{df}R + V_{df} \\ E_q = Ll_f\left(dI_{qf}/dt\right) - \omega Ll_f I_{df} + I_{qf}R + V_{qf} \\ I_{df} = C_f\left(dV_{df}/dt\right) - \omega C_f V_{qf} \\ I_{qf} = C_f\left(dV_{qf}/dt\right) - \omega C_f V_{df} \\ I_{dT} + I_{dC} = I_{df} \\ I_{qT} + I_{qC} = I_{qf} \end{cases} \quad (1)$$

The output current and voltage control are obtained by utilizing feedback/feedforward controls with a PI controller for zero steady-state error, minimizing current error with a fast dynamic response, and maintaining the system stable. The voltage and current controllers with PI controller are expressed as:

$$\begin{cases} E_d = \left(K_{pi} + K_{ii}/s\right)\left(I_{df}^* - I_{df}\right) - \omega C_f I_{qf} + V_{df} \\ E_q = \left(K_{pi} + K_{ii}/s\right)\left(I_{qf}^* - I_{qf}\right) - \omega C_f I_{df} + V_{qf} \end{cases} \quad (2)$$

$$\begin{cases} I_{df} = \left(K_{pv} + K_{iv}/s\right)\left(V_{df}^* - V_{df}\right) - \omega C_f V_{qf} + I_{df} \\ I_{qf} = \left(K_{pv} + K_{iv}/s\right)\left(V_{qf}^* - V_{qf}\right) - \omega C_f V_{df} + I_{qf} \end{cases} \quad (3)$$

4.2 Traditional droop control strategy

For correct load demand sharing, the voltage and frequency droop is used, so physical communication between DGs is not required in this method. Equations (4) and (5) describe the injected active power (P_L) and reactive power (Q_L) delivered by a distributed generator, the voltage E to the terminal V via Z_o impedance (Figure 4):

$$P_L = \left(\frac{EV_o}{Z_o}\cos\delta - \frac{V_o^2}{Z_0}\right)\cos\theta + \frac{EV_o}{Z_o}\sin\delta\sin\theta \quad (4)$$

$$Q_L = \left(\frac{EV_o}{Z_o}\cos\delta - \frac{V_o^2}{Z_0}\right)\sin\theta - \frac{EV_o}{Z_o}\sin\delta\cos\theta \quad (5)$$

δ is the difference in phase between supply and supply terminal, commonly known as power angle, and $Z_o = R_L + jX_L$.

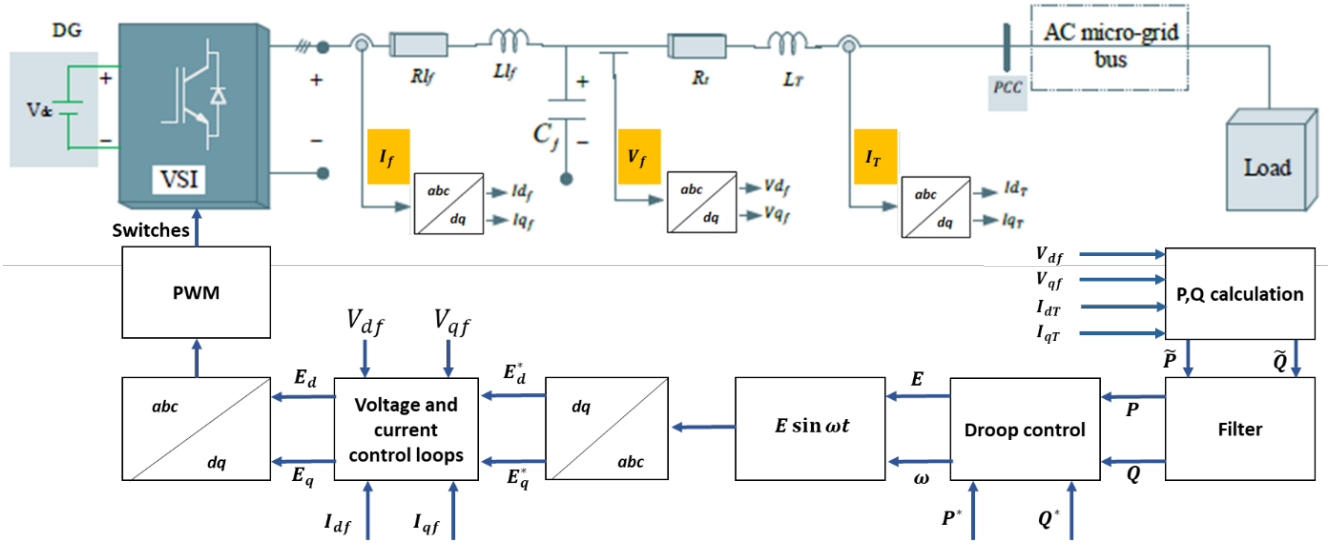

Figure 3. Local controls of the DG

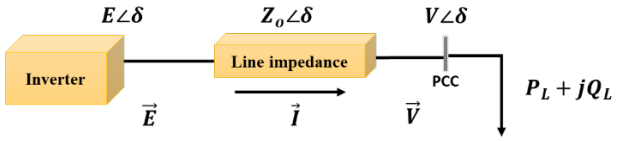

Figure 4. Single DG supplying a load

When using conventional droop control, it is assumed to have inductive dominant lines, thus ($\theta = 90^o$) and we can express the line impedance as,

$$X_L = \omega_o\left(L_{lf} + L_T\right) \quad (6)$$

where ω_o represents the fundamental angular frequency,

$$P_L = VI\cos\theta = \frac{1}{X_L}EV\sin\delta \quad (7)$$

$$Q_L = VI\sin\theta = \frac{1}{X_L}\left(EV\cos\delta - V^2\right) \quad (8)$$

where $\cos\theta$ and δ represent the power factor and power angle respectively, for small power angle $\delta \approx 0$ and $\sin\delta \approx \delta$, whereas $\cos\delta \approx 1$. The later assumptions help us to write equations (7) and (8) as:

$$P_L = \frac{EV}{X_L}\sin\delta \approx \frac{EV}{X_L}\delta \quad (9)$$

$$Q_L = \frac{EV}{X_L}\cos\delta - \frac{V^2}{X_L} \approx \frac{V}{X_L}\left(E - V\right) \quad (10)$$

By differentiating equations (9) and (10), we get,

$$\frac{\partial P_L}{\partial E} = \frac{V}{X_L}\delta, \text{ and } \frac{\partial P_L}{\partial \delta} = \frac{EV}{X_L} \quad (11)$$

$$\frac{\partial Q_L}{\partial E} = \frac{V}{X_L}, \text{and } \frac{\partial Q_L}{\partial \delta} = 0 \quad (12)$$

The Equations (9), (10), (11), and (12) show clearly that $P \sim \delta$ and $Q \sim E$. and the traditional droop control method with inductive dominated lines will take the form:

$$f = f_n^* - m_p\left(P - P^*\right) \quad (13)$$

$$E = E_n^* - n_q\left(Q - Q^*\right) \quad (14)$$

where P^* and Q^* are real and reactive nominal power respectively,

f_n^* and E_n^* are the reference frequency and voltage, respectively,

P and Q are the supplied active and reactive power respectively,

f and E are actual frequency and voltage respectively,

m_p and n_q are the proportional frequency and droop voltage coefficients, respectively.

4.3. The proposed MPC-based arctan droop control method

This control strategy utilizes modified droop control. Instead of using linear droop control, it uses the arctan function in P/f droop control with virtual impedance in the case of inductive dominated MG for primary control of frequency, voltage and reduce the impedance line mismatch for adequate power-sharing. The control strategy also replaces the inner control (Voltage and current control loops) with FCS-MPC as a secondary control for lowering the deviations of the voltage and frequency from their nominal values. The latter one also chooses the proper optimum switching to select the optimum voltage. Figure 5 shows all the control procedure for the MG. The arctan droop control equation is given by:

$$f = f_{nom} - \frac{a_p}{\pi} * Arctan\left(\rho\left(P - P_{ref}\right)\right) \quad (15)$$

$$v_{droop} = V_{nom} - n_q * \left(Q - Q_{ref}\right) \quad (16)$$

where ω_{nom} is nominal frequency, V_{nom} is the nominal voltage, P_{ref} is reference active power, Q_{ref} is reference reactive power, i_f is inductor filter current, $v_o = v_c$ is the output voltage, i_o is output current, v_{ref} is output voltage reference droop with virtual impedance, and v_{droop} denotes the droop voltage. a_p is constant for controlling the bounds, m_q is the droop coefficient, ρ is a constant for controlling the concavity.

The following equations, respectively, give the virtual impedance and its voltage drop equation:

$$z_v = R_v \mp \frac{\omega_c s L_v}{s + \omega_c} \quad (17)$$

$$v_{zv} = i_o * z_v \quad (18)$$

The reference voltage is now expressed by the equation below:

$$v_{ref} = v_{droop} - v_{zv} \quad (19)$$

where L_v is a virtual inductance; $\omega_c/(s + \omega_c)$ represents low pass filter; and R_v represents virtual resistance.

The inputs of FSC-MPC are the output from reference voltage after the introduction of the virtual impedance loop, the measured filter current, and measured capacitor filter voltage, as shown in Figure 6. The block diagram of the FCS-MPC in conjunction with the arctan droop control algorithm for a three-phase inverter with an output LC filter, considering a one prediction step N = 1, is shown in Figure 7. The control scheme at sampling time k is described step by step as follows:

1. Measure the value of the output voltage $v_c(k)$, the filter current $i_f(k)$ and output current $i_o(k)$ at sampling time k.
2. Detect reference voltage $v_{ref}(k)$ obtained from arctan droop control with virtual impedance (equation 19) and dc-link voltage V_{dc}
3. Predict the value of the output voltage at the next sampling instant $v_c(k+1)$ for all the possible voltage vectors that the inverter generates.
4. The seven predictions obtained for $v_c(k+1)$ are compared with the reference voltage $v_{ref}(k)$ (obtained in step 2) using a cost function g, as shown in Figure 7.
5. The voltage vector V_t that minimizes this function is then chosen and its corresponding switching state is applied at the next sampling instant.
6. Wait until sampling time k+1 and turn back to step 1.

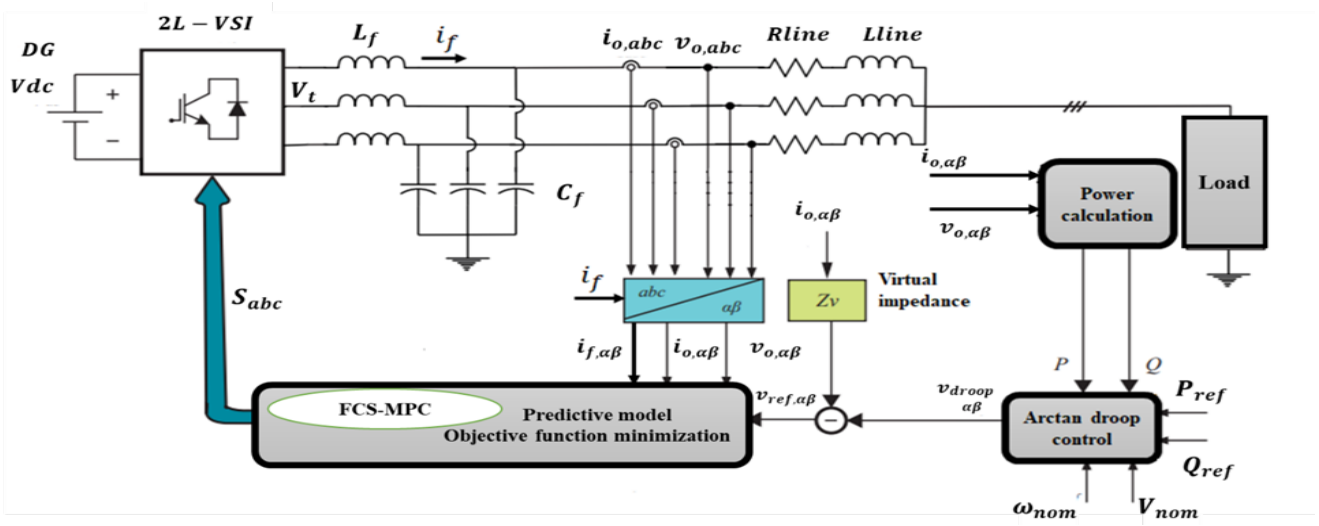

Figure 5. MPC-based arctan droop control method

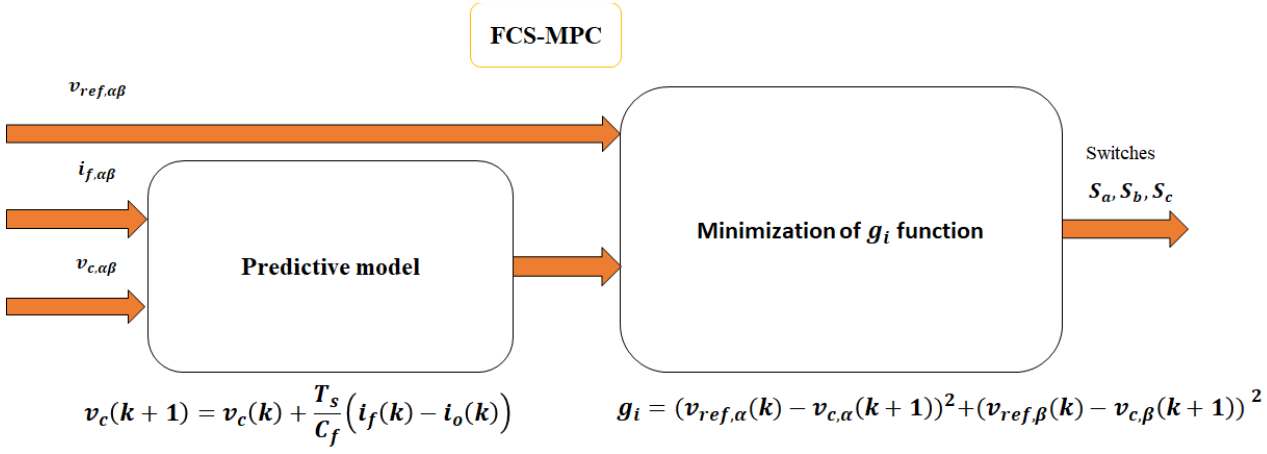

Figure 6. FSC-MPC control diagram

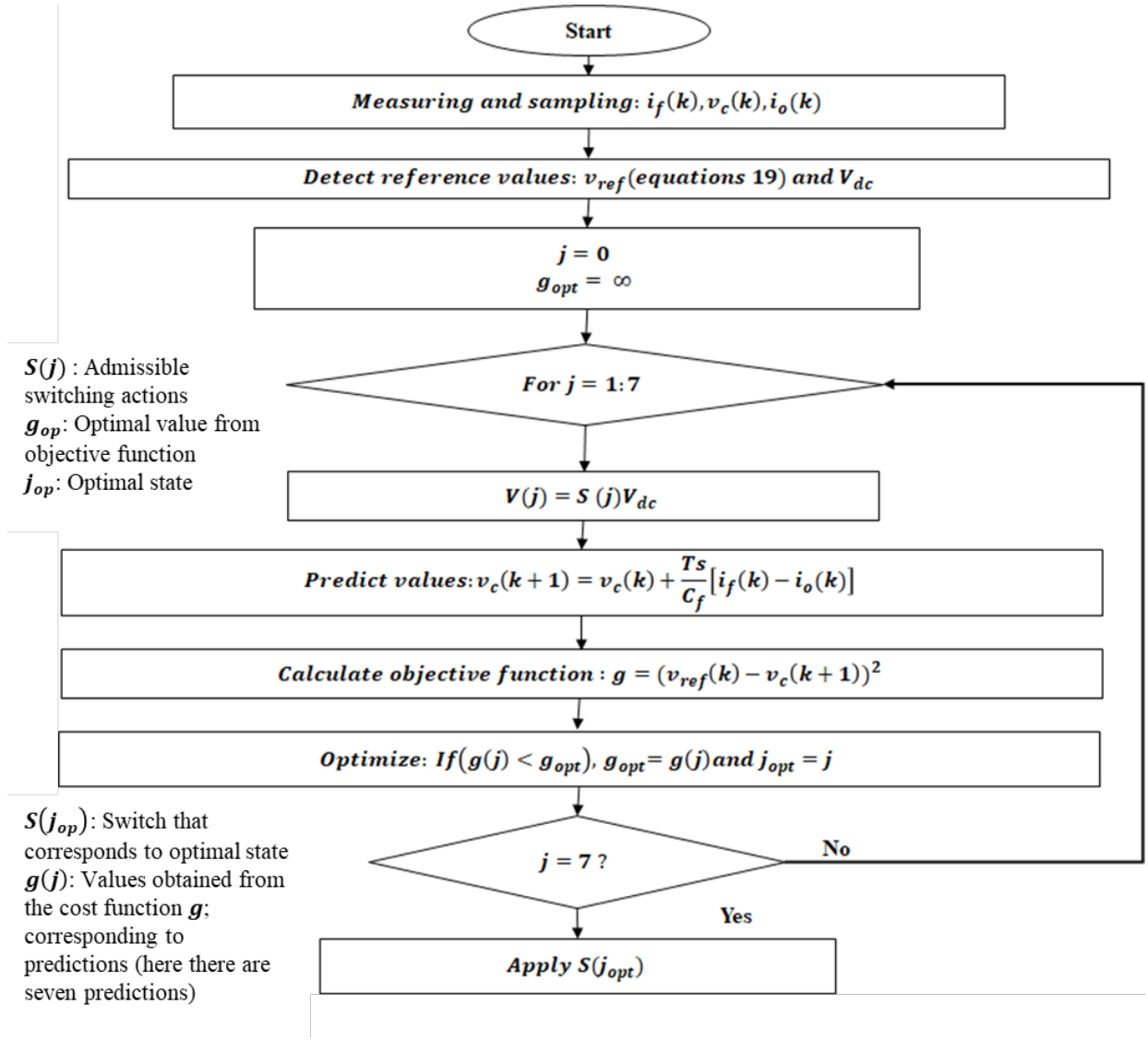

Figure 7. FSC-MPC in conjunction with arctan droop control algorithm

4.4. Comparative evaluation criteria

The comparative evaluation considers criteria like checking the power ratio if they are compatible with microsource output concerning load supplied, evaluating reactive and active power sharing errors caused by the feeders' mismatched output impedances. When there is a difference in voltage source inverters' output impedance, voltage deviations and frequency fluctuations occur. The power errors caused by this effect are analyzed.

Reactive and active power errors are evaluated as follows:

$$e_{pi} = \frac{P_i^* - P_i}{P_i^*} \times 100\% \quad (20)$$

$$e_{Qi} = \frac{Q_i^* - Q_i}{Q_i^*} \times 100\% \quad (21)$$

where

P_i^*: The active power supplied by the i^{th} inverter in case of active power-sharing with exact proportion to the ratings

Q_i^*: The reactive power supplied by the i^{th} inverter in case of reactive power-sharing with exact proportion to the ratings

P_i: Measured active power supplied by the i^{th} inverter

Q_i: Measured reactive power supplied by the i^{th} inverter

The active and reactive power sharing ratios are calculated as follows:

$$\begin{cases} \frac{m_1}{m_2} = \frac{P_2}{P_1} = \ldots = \frac{m_k}{m_{k+1}} = \frac{P_{k+1}}{P_k} \\ \frac{n_1}{n_2} = \frac{Q_2}{Q_1} = \ldots = \frac{n_k}{n_{k+1}} = \frac{Q_{k+1}}{Q_k} \end{cases} \quad (22)$$

where

m, n : are active and reactive power droop coefficients respectively

P, Q : Active and reactive power delivered by microsources in active and reactive power sharing with exact power ratio and droop coefficients.

5. Results and discussions

In this part, two DGs based inverter are connected in parallel to supply a linear load through different impedance lines, as depicted in Figure 8. The MPC-based droop control strategy's performance to regulate inverters for voltage and frequency stabilization in a microgrid is compared to the traditional droop control strategy. Only an islanded mode is considered for this analysis. Apart from the steady-state analysis, the sudden load change is introduced for the transient analysis during the studied system's operation. In the normal operation mode, all parallel inverters and load 1 are always connected to PCC. At time 0.4s, load 2 is connected to PCC. Again the load 2 is disconnected from the grid at time 0.8 s. Table I. summarizes the data used in this paper.

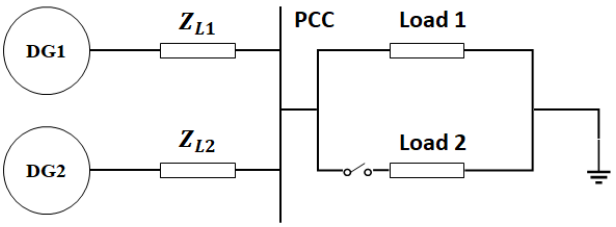

Figure 8. Microgrid with paralleled DGs and loads [18]

5.1. Comparative evaluation of MPC-based arctan droop controller (proposed) versus conventional droop control

The comparative evaluation of the control strategies is shown in Figures 9-12. Figure 9 shows the frequency variation by using two different control methodologies. The results showed that frequency is much more controlled using the proposed control strategy where the variation range was 49.98-49.99 Hz compared to 49.92- 49.96 Hz for the conventional droop control. In all scenarios, it takes 0.025 s for the frequency to stabilize for the proposed control scheme, whereas for the traditional droop control method, the time to stabilize is 0.1 s, as shown in Figure 9. The voltage deviations between the two inverters when using the conventional control strategy and the proposed control strategy were compared. Figure 10 shows the voltage variations for both methods. At times 0-0.4s, 0.4-0.8s, and 0.8-1.2 s, the voltage deviations were 1.3V, 2.7V, and 1.3V, respectively, when using the conventional droop. On the other hand, the voltage deviations during the same events were 0.003V, 0.005V, and 0.003V when using the proposed control method. This large voltage deviation in conventional droop control causes unequal reactive power-sharing. The voltage stabilization time is 0.05s in all events when the proposed control strategy is used, compared to 0.1s for the traditional droop control scheme, as observed in Figure 10. The proposed method demonstrated very low deviations between the inverters compared to the conventional droop control method. This better performance of the proposed method for voltage and frequency control is due to the fictitious impedance loop's insertion, which removes the impedance disparities between the inverters and the MPC method to track the reference voltage. The output voltage and frequency for the inverters remained in the allowable range of variation according to IEEE 1547-2018 standards using both methods.

The active and reactive power sharing comparisons of the two methods are explained in Figures 11-12. The results showed that for the proposed control strategy, the active power-sharing ratio is P1:P2=1:1, which means that the DGs share the load at 50% each. In traditional droop control, the DG1 and DG2 supply the load at the active power-sharing ratio of P1:P2=1:1, which is 49.8% and 49.8% of the load's total active power, respectively, as shown in Figure 11. Figure 12 highlights the reactive power-sharing comparisons between the studied control strategies.

Table 1. System test data

Parameter	Value
DC bus voltage	850 V
Nominal bus frequency	50 Hz
Nominal voltage	400 V
Line impedance, DG1	30.25 mH, 0.0805 Ω
Line impedance, DG2	48.4 mH, 0.1288 Ω
Load 1	6000W, 1500VAr
Load 2	6000W, 1500VAr
Droop coefficients, DG1	$\rho_1 = 8.75e-5\ V/W$, $n_{q1} = 25e-4\ rad/sVAr$
Droop coefficients, DG2	$\rho_2 = 8.75e-5 V/W$, $n_{q2} = 25e-4\ rad/sVAr$
Sampling time	Ts = 30us
Bounds control coeficient	$a_{p1} = a_{p2} = 1$
Virtual impedance	$R_{v1} = 0.0483\ \Omega$, $L_{v1} = 18.15\ mH$
The allowable frequency range of variation	50 Hz +/-1%
The allowable voltage range of variation	400 V +/- 5%
Pmax, Qmax	8kW, 6kVAr
Filter	Lf=3e-3H, Cf=15uF
Inner loops PI coefficients for conventional droop control	Kpi=0.15,Kii=1.5 Kpv=20, Kiv=1000
Inverter switching frequency	5kHz

It has been found that the proportionate reactive power-sharing using the proposed control strategy is achieved, and both DG units share the load approximatively at a percentage of 50% each. It is not the same case in traditional droop control, where DG1 delivered 66.33%, and DG2 supplied 33.64% of the total reactive power of the load.

This better performance of the proposed method for power-sharing is explained by its capability to reduce the effect of line impedance mismatch among the DG units based inverters, tracking the reference voltage that boosts proportionate power-sharing among DGs in the microgrid. The analysis is also done on the comparative evaluation of reactive and active power errors. The results revealed that the proposed control method's performance is superior to the conventional droop control because the proposed control strategy presented low power errors over the traditional droop control. The comparisons are summarized in Table 2.

Table 2. Performance comparison of studied control strategies based on power errors

Control method	$e_{p1}(\%)$	$e_{p2}(\%)$	$e_{q1}(\%)$	$e_{q2}(\%)$
Conventional droop control	4.85	4.82	-24.27	34.33
MPC-based arctan droop control (proposed)	0.05	-0.03	-0.05	0.033

6. Conclusion

Parallel connected inverters must keep the same voltage and output impedances to ensure active and reactive power-sharing. Unequal output impedances of VSIs leads to disproportionate reactive power-sharing and poor voltage regulation when conventional droop control is used. The proposed MPC-based arctan droop control overcomes these drawbacks and has been found to give reduced settling and response times relative to conventional droop control methods. The results showed that proportionate power-sharing of DG units with unequal line impedance is ensured when the proposed strategy is utilized, in contrast to the traditional droop controller, which can vary. The findings showed that the proposed MPC-based arctan droop control had improved control over voltage and frequency.

Future work will focus on implementing the two-step prediction FSC-MPC with arctan droop control and evaluating its effect on voltage and frequency control in VSIs-based microgrids. The proposed control technique will be extended to cater for microgrids with a higher degree of control and a broad microgrid-benchmark.

Acknowledgments

This research was supported by the Pan African University, Institute for Basic Sciences, Technology and Innovation in the form of postgraduate student research funding

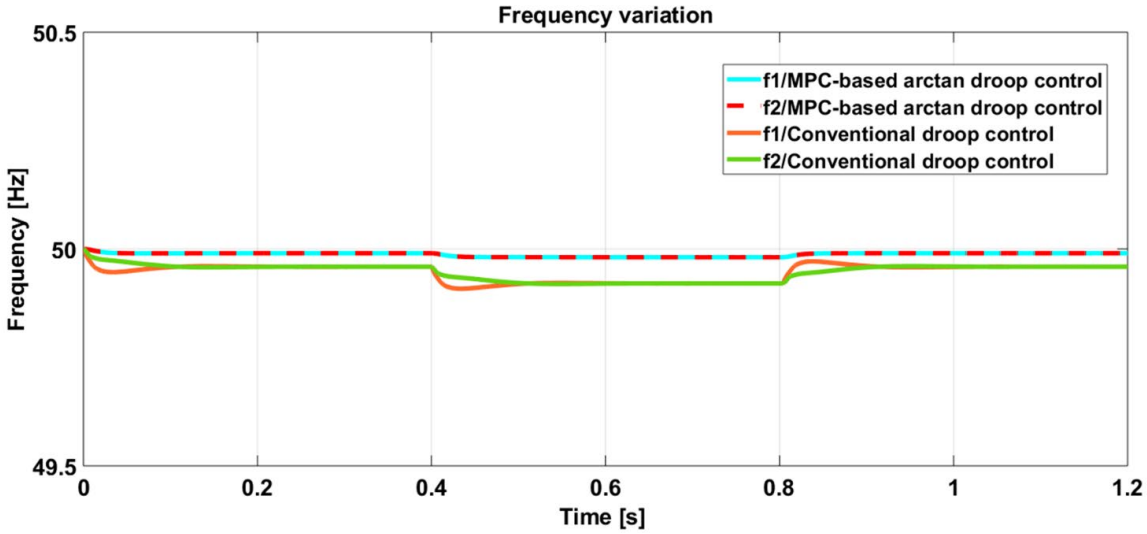

Figure 9. Comparative evaluation for frequency using proposed method versus conventional droop control

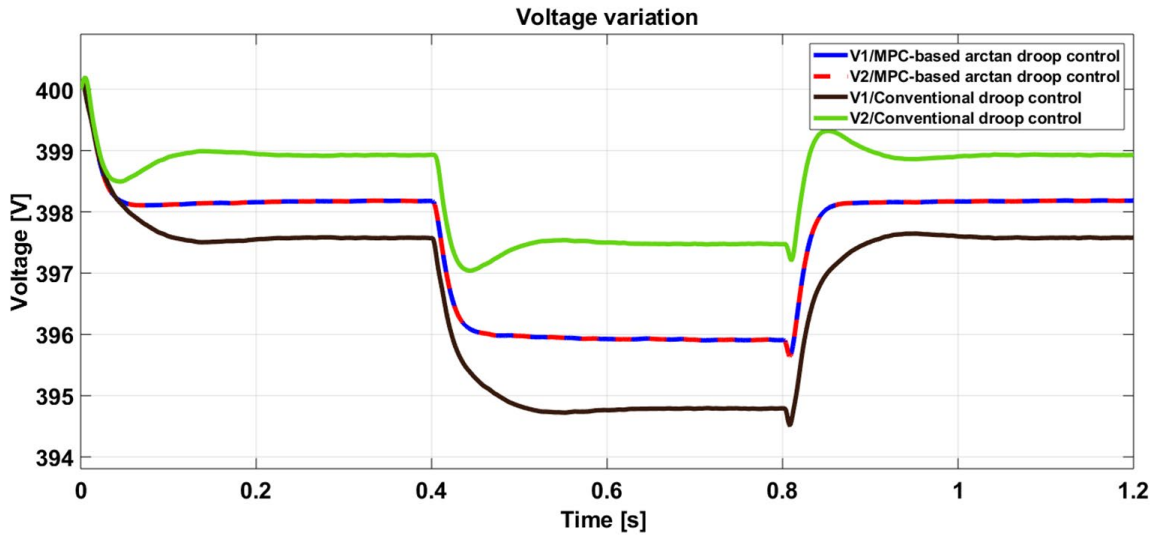

Figure 10. Comparative evaluation for voltage using proposed method versus conventional droop control

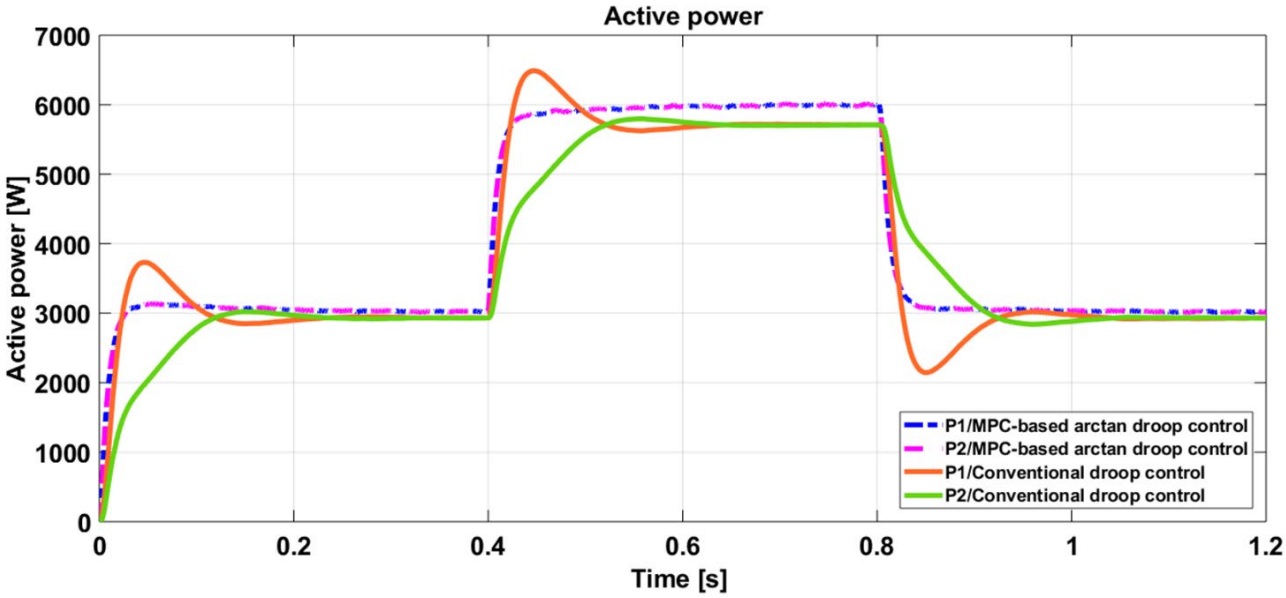

Figure 11. Active power-sharing using the proposed control strategy versus conventional droop control

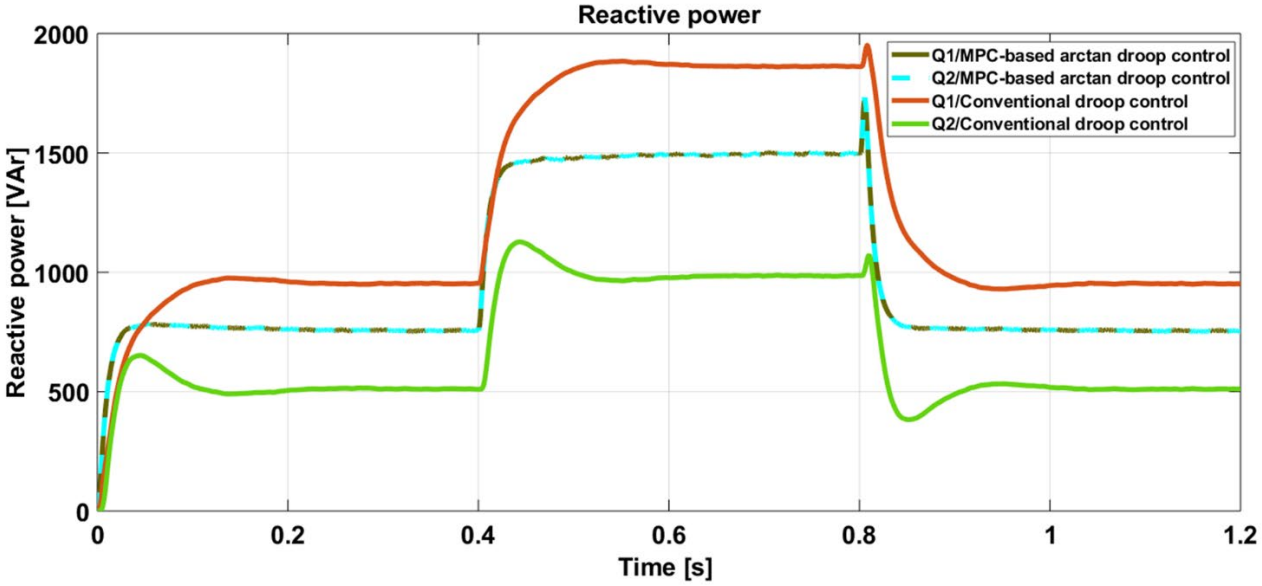

Figure 12. Reactive power-sharing using the proposed control strategy versus conventional droop control

References

[1] H. Gu, D. Wang, H. Shen, W. Zhao, and X. Guo, "New Power-Sharing Control for Inverter-Dominated Microgrid Based on Impedance Match Concept," Sci. World J., pp. 1–7, 2013.

[2] A. El, M. Bouzid, and P. Sicard, "Simulation of Droop Control Strategy for Parallel Inverters in Autonomous AC Microgrids," 8th Int. Conf. Model. Identif. Control, 2016, pp. 701–706.

[3] Q. Fu et al., "Microgrid generation capacity design with renewables and energy storage addressing power quality and surety," IEEE Trans. Smart Grid, vol. 3, no. 4, pp. 2019–2027, 2012.

[4] V. Monteiro, J. Catalao, T. Sousa, J. G. Pinto, M. Mezaroba, and J. L. Afonso, "Improved voltage control for the electric vehicle operation in V2H mode as an off-line UPS in the context of smart homes," EAI Endorsed Trans. Energy Web, vol. 7, no. 25, pp. 1–8, 2020.

[5] J. M. Guerrero, M. Chandorkar, T. L. Lee, and P. C. Loh, "Advanced control architectures for intelligent microgrids part- I: Decentralized and hierarchical control," IEEE Trans. Ind. Electron., vol. 60, no. 4, pp. 1254–1262, 2013.

[6] U. B. Tayab, M. A. Bin Roslan, L. J. Hwai, and M. Kashif, "A review of droop control techniques for microgrid," Renew. Sustain. Energy Rev., vol. 76, no. 3, pp. 717–727, 2017.

[7] K. Manjunath and V. Sarkar, "Performance assessment of different droop control techniques in an AC microgrid," 7th International Conference on Power Systems, ICPS, 2018, pp. 93–98.

[8] E. H. Margoum, N. Krami, L. Seca, C. Moreira, and H. Mharzi, "Design and control of parallel three-phase voltage source inverters in low voltage AC microgrid," Adv. Electr. Electron. Eng., vol. 15, no. 2, pp. 120–129, 2017.

[9] J. W. Simpson-Porco, F. Dörfler, and F. Bullo, "Voltage Stabilization in Microgrids via Quadratic Droop Control," IEEE Trans. Automat. Contr., vol. 62, no. 3, pp. 1239–1253, 2017.

[10] Y. Hennane et al., "Power Sharing and Synchronization Strategies for Multiple PCC Islanded Microgrids," international J. Electr. Electron. Eng. Telecommun., vol. 9, no. 3, pp. 156–162, 2020.

[11] T. Chen, O. Abdel-Rahim, F. Peng, and H. Wang, "An Improved Finite Control Set-MPC-Based Power Sharing Control Strategy for Islanded AC Microgrids," IEEE Access, vol. 8, pp. 52676–52686, 2020.

[12] A. E. M. Bouzid, P. Sicard, H. Chaoui, A. Cheriti, M. Sechilariu, and J. M. Guerrero, "A novel Decoupled Trigonometric Saturated droop controller for power-sharing in islanded low-voltage microgrids," Electr. Power Syst. Res., vol. 168, no. 7, pp. 146–161, 2019.

[13] T. Dragicevic, "Model Predictive Control of Power Converters for Robust and Fast Operation of AC Microgrids," IEEE Trans. Power Electron., vol. 33, no. 7, pp. 6304–6317, 2018.

[14] A. J. Babqi and A. H. Etemadi, "MPC-based microgrid control with supplementary fault current limitation and smooth transition mechanisms," IET Gener. Transm. Distrib., vol. 11, no. 9, pp. 2164–2172, 2017.

[15] U. B. Tayab and Q. M. Humayun, "Enhanced droop controller for operating parallel-connected distributed-generation inverters in a microgrid," J. Renew. Sustain. Energy, vol. 10, no. 4, 2018.

[16] C. N. Rowe, T. J. Summers, R. E. Betz, C. N. Rowe, T. J. Summers, and R. E. Betz, "Arctan Power Frequency Droop for Power Electronics Dominated Microgrids Arctan power frequency droop for power electronics dominated microgrids *," Aust. J. Electr. Electron. Eng., vol. 10:2, no. 11, pp. 157–165, 2013.

[17] Y. Shan, J. Hu, Z. Li, and J. M. Guerrero, "A Model Predictive Control for Renewable Energy Based AC Microgrids Without Any PID Regulators," IEEE Trans. Power Electron., vol. 33, no. 11, pp. 9122–9126, 2018.

[18] C. Dou, Z. Zhang, D. Yue, and M. Song, "Improved droop control based on virtual impedance and virtual power source in low-voltage microgrid," IET Gener. Transm. Distrib., vol. 11, no. 4, pp. 1046–1054, 2017.